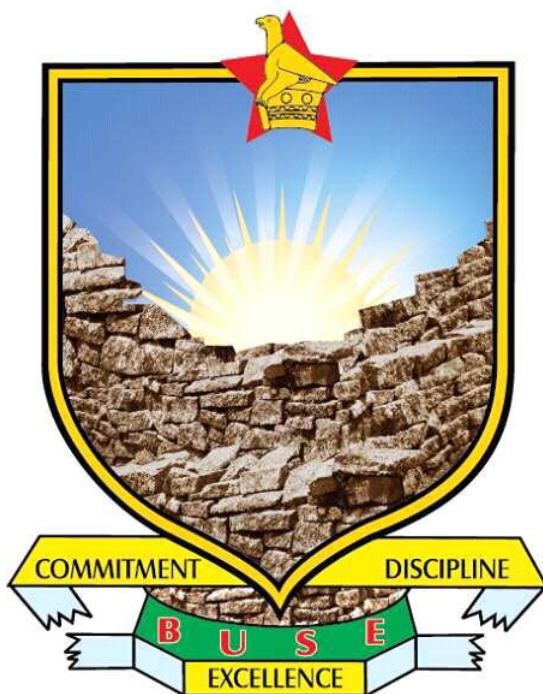**BINDURA UNIVERSITY OF SCIENCE EDUCATION**

FACULTY OF SCIENCE AND ENGINEERING

CHEMISTRY DEPARTMENT

Extraction of Silica and synthesis of silicon from corn cob ashes

BY

MDOKA DARREN KONDWANI (B1850398)

NOVEMBER 2022

SUPERVISOR: PROF MUPA

A DISSERTATION SUBMITTED IN PARTIAL FULFILMENT OF THE REQUIREMENTS OF THE BACHELOR OF SCIENCE HONOURS DEGREE IN CHEMICAL TECHNOLOGY (HBSc CHT)

APPROVAL FORM

The undersigned certify that they have supervised, read and recommend to the Bindura University of Science Education for the acceptance of a research dissertation entitled:

Submitted by Mdoka Darren Kondwani (B1850398)

In the partial fulfilment of the requirements for the Bachelor of Science Education Honours Degree in Chemical Technology (HBSc.Chem.Tech).

(Student signature) …………………………. Date …………………………………….

(Supervisor signature) …………………………... Date…………………………………...

(Chairperson Signature) …………………………... Date…………………………………...

DECLARATION

I, Darren Kondwani Mdoka, do hereby declare to Bindura University of Science Education that this dissertation is my original work and all materials and academic sources of information other have been duly acknowledged. This work has not been submitted to any other academic institution for the purposes of an academic merit.

(Student signature) ……………………………. Date …………………………………….

ACKNOWLEDGEMENTS

DEDICATION

To my family and friends.

ABBREVIATIONS and ACRONYMS

SEM   Scanning Electron Spectroscopy

TEM   Transmission Electron Microscope

XRD   X-ray Diffraction

XRF   X-ray Fluorescence

FTIR   Fourier Transform Infrared

NTP   National Toxicology Program

OSHA   Occupational Safety and Health Administration

SCBA   Sugarcane Bagasse Ash

CCA   Corn Cob Ash

Table of Contents

ABSTRACT

This research investigated the use of corn cob waste as a source of silica and the potential of corn cob ash as a precursor in the extraction of silica, which can be reduced to silicon. According to this research, burning corn cob ashes resulted in the production of silica through an extraction process, which lessened the environmental impact of ash disposal issues. Ash content of corn cob ashes that were produced after burning the corn cob refuse at various temperatures (700°C, 800°C, and 900°C) for three hours was assessed. Sulphuric acid was used to wash the corn cob ash in order to get rid of any impurities and metal ions and so as to obtain silica, a precursor used in the synthesis of silicon, an alkaline extraction technique was used, followed by reduction of silica using magnesium and zinc. For samples 1, 2, and 3, the percentage output for the silica gel obtained was 30%, 26%, and 23%, respectively. Samples 1, 2, and 3 had silicon percentages of 54%, 42%, and 39%, respectively.

LIST OF TABLES

LIST OF FIGURES

CHAPTER 1: INTRODUCTION

1.1 BACKGROUND

Zea mays L., sometimes known as maize, is a cereal grain that was first domesticated by native peoples in southern Mexico. The plant's leafy stem produces pollen inflorescences and distinctive ovuliferous inflorescences known as ears, which, upon fertilization, develop into kernels or seeds that become fruits (Ajayi-Owoeye et al 2015). With maize production outpacing that of wheat and rice, it has become a common food in many parts of the world. In addition to being consumed directly by people, maize is also used to make corn ethanol, animal feed, and other goods like corn starch and corn syrup. The cob is a waste product from all of this. As a by-product of the maize crop, maize cobs are the fibrous core of the female inflorescence, also known as the maize ear. The term "maize cob" often refers to the complete maize ear, with or without the grains and husks, however this study solely examines the maize cob without the grains. (Handayani-Rahmawati et al, 2021) asserts that the fiber lignocellulose material from the stalks, hemicellulose, ash, and wax are the main components of sugarcane bagasse. The abundance of solid agricultural waste leftovers poses a disposal risk to the environment due to the development of odors, insect attraction, and soil deterioration. Utilizing biomass for energy instead of coal, such as leftover corn cobs and other agricultural waste, may help ease environmental concerns like pollution. One sort of agricultural waste that might be used as a natural silica source is corn cobs.

The main use for corn cobs is as field manure. The species and age of the maize cobs, the geological and soil conditions, the fertilizer used, and the farming method, according to (Mohanraj et al. 2018), all affect the quantity of silica in corn cob ash (Chindaprasirt & Rattanasak, 2020). High levels of silica in corn cob ash make it a valuable product with a variety of potential uses, including the production of silica gel for adsorbency, as a raw material for ceramics, as an additive for cement and concrete, as a catalyst, in cosmetics, paint and coating, as a reinforcing agent in the rubber industry, as a cleaning agent in toothpaste, as an anticaking agent in salts, in cosmetics, and so on. In this article, methods to economically recover silica from waste ash are reviewed. This not only increases value but also addresses the issue of how to dispose of copious amounts of corn cob ash. An alkaline extraction technique for manufacturing silica from agricultural waste containing silica, is employed in this case to create high grade amorphous silica.

Figure 1.1 (a) and (b) Maize cobs without kernels and (c) maize cobs with corn kernels

1.2 AIM

The study aims to synthesize silicon from corn cob ash and determine the viability of the production process.

1.3 OBJECTIVES

- To synthesize silica from corn cob biomass ash.
- To synthesize silicon from silica via the magnesium reduction route.
- To evaluate the effect of different synthesis parameters on the yield of silicon.
- To characterize corn cob ash, silica and silicon.
- To suggest a process flow for the production of silicon from corn cob ash.

1.4 STATEMENT OF PROBLEM

In terms of biomass, Zea mays L produces not just cereal grains but also corn cobs, stalks, and dry leaves that may be used as chemical feedstock and energy sources.

The stalk makes up the majority of the biomass wastes from maize production, which ranges from 60 to 70 percent wastes (Schollbach and Brouwers, 2019). The ash produced by burning maize cobs as fuel is seen to be waste and causes disposal issues, which lessens the impact on the environment. This study will demonstrate how burning maize cobs results in the extraction of silica and the further separation into silicon, a valuable chemical. In this article, ash from maize cobs will be used to make silica. Due to its naturalness, affordability, availability, recyclability, low toxicity, and high silica content, corn cob has been used as the primary source of silica. This so appears to bring up a variety of options for producing silicon precursors from corn cob ash.

1.5 SIGNIFICANCE OF STUDY

- Corn cob ash is readily available therefore the raw materials are readily available.

- Producing silica from corn cob by-product and further producing silicon from this residue waste alleviates land and water pollution.
- In this investigation silica is being made from waste, this entails one can use cheaper products and reduce the cost of purchasing expensive industrial products.
- The study is therefore of paramount importance as it will not only reduce land pollution and will help in preserving human, aquatic and bird life.

1.6   SCOPE OF THE STUDY

The research will examine the production of silica and silicon from biomass maize waste, with a particular emphasis on the corn cob. Following its production, silica and silicon will be examined for its thermodynamic and kinetic properties, as well as its FT-IR characteristics.

CHAPTER 2: LITERATURE REVIEW

2.1 INTRODUCTION

This chapter's main focus is on the evaluation of the requisite theory and the related labor needed to put this research together. The chapter also attempts to describe the earlier study conducted by other researchers, as well as their ideas and useful contributions to the production of silica from corn cob ash and further extraction of silicon from the silica.

2.2 CHEMICAL STRUCTURE, PROPERTIES AND REACTIONS OF SILICON

A glistening greyish tetravalent non-metallic crystal that makes up 27% of the Earth's crust, silicon is an element with atomic symbol Si and is considered a close relative of carbon (Bhardwaj et al., 2018). Silicon possesses numerous polymers such as silicides, silica, halides (silicon tetrahalides), silicate minerals and silicic acids. Silicon is found attached to other elements for example in silica each silicon atom in silica is normally bonded to four oxygen atoms (Hamouda & Amiri, 2014). Most of the silicon used in our everyday life exists as metal silicates and developments have been made in extraction of these silicates from various sources taking into account the salt sodium silicate which is a polymeric anion which has silicate as the counter-ion and both the sodium and silicate ions are present in the inorganic sodium salt known as sodium silicate, which dissolves in water to create alkaline solutions. The specific mechanism for the synthesis of sodium silicate is formed when silica reacts with an alkaline, such as sodium hydroxide. In alkaline and neutral fluids, sodium silicate is stable. Silicate ions, on the other hand, combine with hydrogen ions in acidic solutions to generate silicic acids, which are likely to break down into hydrated silicon on the dioxide gel. It becomes harder and more transparent when heated further, becoming silica gel (Ali & Amiri, 2014).

Figure 2.1 Silicon metal
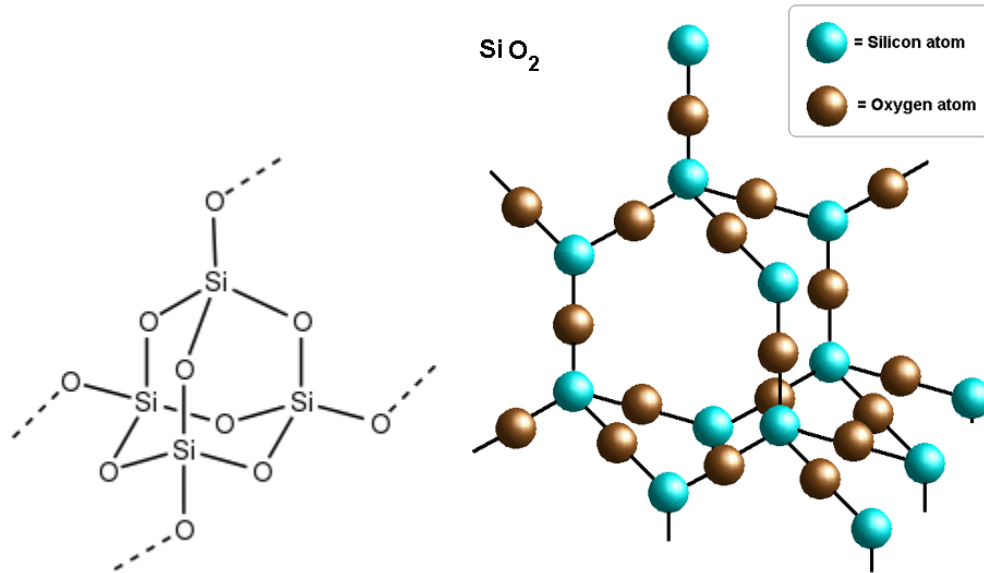
Figure 2.2 Structural representation of silica SiO_2

2.3   METHODS FOR THE REDUCTION OF SILICA TO SILICON

2.3.1   Aluminothermic reduction

Aluminothermic reduction is the name given to this reduction process, which uses aluminum as the reducing agent. Aluminum can convert silicon dioxide to create silicon because it is a more active metal than silicon. Such an exothermic reaction can be sustained by the quick spread of a combustion front without the need for additional energy. For the creation of composite materials, aluminothermic reduction has been proposed. It has been proposed to use aluminothermic reduction with a mixture of Al and SiO_2 to create alumina-aluminum-silicon composite materials (Wang and Shi, 2017).

$$3SiO_2 + 4Al \longrightarrow 2Al_2O_3 + 3Si$$
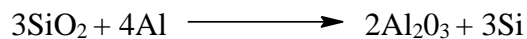
It is possible to use this process to produce silicon. The creation of mullite and the reduction of silicon from mullite can occur via two further reactions once alumina has been created through the aforementioned reaction in the presence of silica:

$$3Al_2O_3 + 2SiO_2 \longrightarrow Al_6Si_2O_{13}$$

$$8Al + 3Al_6Si_2O_{13} \longrightarrow 13Al_2O_3 + 6Si$$
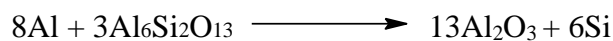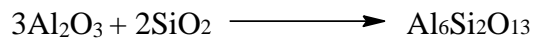
2.3.2   Carbothermic reduction

Quartz can be reduced at high temperatures with carbon while containing silicon. The production of silicon (of the metallurgical grade) currently takes place in an electric arc furnace that uses a

carbothermic process. In this procedure, the furnace is charged with quartz rock and a variety of reducing agents, including coke, coal, and wood chips, and the temperature is raised by an electric arc to 2400K (2127°C). When silica and carbon react, silica is decreased. To complete the reduction process, the following intermediary reactions take place (Lynch, 2015):

$$SiO_2 (l) + Si (l) \longrightarrow 2SiO (g)$$

$$SiO (g) + 2C(s) \longrightarrow SiC(s) + CO (g)$$

$$SiO (g) + SiC(s) \longrightarrow 2Si (l) + CO (g)$$
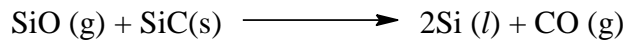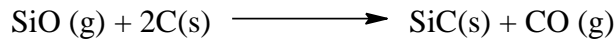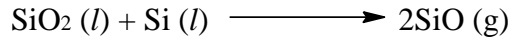
The main source of various contaminants in the finished product in this process, and the reason for its low purity level, is the reductant mixture, which consists of lignite, petroleum-coke, charcoal, and wood chips. In addition to premium quartz, charcoal is also used in Brazil as a reducing agent in the production of metallurgical silicon. This is reflected in the quality of Brazilian metallurgical silicon, which can achieve a purity of up to 99.88% when processed under strict control and using high-quality raw materials (Pires et al., 2018).

2.3.3 Magnesiothermic reduction

Silica (SiO_2) can be reduced by magnesium to produce silicon through the following reaction:

$$SiO_2 + 2Mg \longrightarrow 2MgO + Si$$

The reaction may involve formation of Mg_2Si in the early stages followed by reduction of SiO_2 by Mg2Si through the following chemical reactions:

$$SiO_2(s) + 4Mg (g) \longrightarrow 2MgO(s) + Mg_2Si(s)$$

$$Mg_2Si(s) + SiO_2(s) \longrightarrow 2MgO(s) + 2Si(s)$$
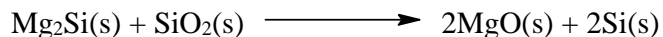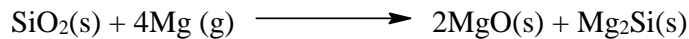
In the presence of excess Mg in the reactants, more Mg_2Si may form by consuming elemental silicon through the reaction:

$$Si(s) + 2Mg (g) \longrightarrow Mg_2Si(s)$$
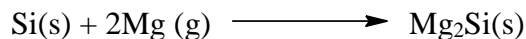
At 650°C, which is the melting temperature of magnesium, Bao et al. (2014) reported converting diatom frustules (SiO_2) to porous nanocrystalline silicon using Mg vapour. In this instance, silica particle reduction from the surface to the interior produced a mixture of MgO and Si.

The silicon product was significantly prevented from becoming coarser and sintering due to the relatively low reduction temperature of 650°C and the development of MgO phases entangled with the silicon product (Bao et al., 2014). However, due to exothermic reactions that result in extreme

temperatures and the formation of magnesium silicide (Mg_2Si) with Si product, the magnesiothermic approach has not found widespread industrial application (Zulumyan et al., 2016).

2.3.4 Calciothermic reduction

The reduction of calcium is analogous to the reduction of aluminium. Mishra et al. (2015) conducted a study on the Calciothermic method that converts amorphous silica (obtained from rice husk) into silicon of reasonable purity. As a result, the following reaction occured:

$$SiO_2 + 2Ca \longrightarrow 2CaO + Si$$
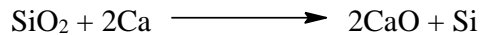
At $720^{o}C$, calcium reduced amorphous silica to silicon. After acid leaching with concentrated HNO_3 and HF, Mishra et al. (2015) reported that the final purity of silicon was 99.9%.

2.4 Environmental Effects

Elemental silicon can be inhaled, swallowed, or come into contact with the skin or eyes, exposing workers to it in these ways. In the latter two scenarios, silicon provides a little irritation risk. If inhaled, it is dangerous. The legal limit for silicon exposure in the workplace is 15 mg/m^3 total exposure and 5 mg/m3 respiratory exposure for an eight-hour workday, according to the Occupational Safety and Health Administration (OSHA). Over the course of an eight-hour workday, the National Institute for Occupational Safety and Health (NIOSH) has established a recommended exposure limit (REL) of 10 mg/m3 for total exposure and 5 mg/m^3 for respiratory exposure. Silicosis is an occupational lung disease characterized by inflammation and scarring in the form of nodular lesions in the upper lobes of the lungs after exposure to crystalline silica dust.

2.5 APPLICATIONS OF SILICON

2.5.1 Alloys

As ferrosilicon or silicocalcium alloys, elemental silicon is added to molten cast iron to enhance performance in casting thin sections and prevent cementite formation where exposed to the atmosphere. The presence of elemental silicon in molten iron functions as an oxygen sink, allowing for more precise control of the steel's carbon content, which must be kept within specific ranges for each form of steel. Although this form of elemental silicon is incredibly impure, it makes up 80% of all free silicon used worldwide and serves as a gauge for the steel industry. Silicon plays a significant role in the composition of electrical steel, altering its ferromagnetic and resistivity characteristics. Silicon's characteristics can be exploited to alter alloys made with metals other than iron. "Metallurgical grade" silicon has a purity level of 95-99%. According to Kamal.Y et al (2022)

approximately 55% of the world's metallurgical purity consumption for the manufacturing of aluminum-silicon alloys (silumin alloys) used mostly in the automotive industry, silicon is used. Because silicon makes up a large portion (12%) of the eutectic mixture that solidifies with very little thermal contraction, silicon is crucial in the casting of aluminum. This significantly lessens tearing and cracks that result from stress as casting alloys solidify after cooling. Additionally, silicon considerably raises the hardness and consequently the wear resistance of aluminum (Kamal Y et al..,2022).

2.5.2 Electronics

In common integrated circuits, a monocrystalline silicon wafer serves as a mechanical support for the circuits, which are created by doping and insulated from each other by thin layers of silicon oxide. The silicon oxide insulator, silicon oxide, is easily produced on silicon surfaces by processes of thermal oxidation or local oxidation (LOCOS), which involve exposing the element to oxygen under the proper conditions that can be predicted by the Deal-Grove model (Dekker et al ,2022). The properties of silicon can be used to modify alloys made of metals other than iron. The purity of "metallurgical grade" silicon ranges from 95 to 99%. Approximately 55% of the world's usage of metallurgical purity Silicon is utilized in the production of aluminum-silicon alloys (silumin alloys), which are mostly employed in the automotive industry. Silicon is essential in the casting of aluminum because it makes up a sizable amount (12%) of the eutectic mixture that solidifies with very little thermal shrinkage. As casting alloys consolidate after cooling, this considerably reduces the stress-related tearing and cracking that occurs. Additionally, silicon significantly increases the hardness of aluminum, which in turn increases its wear resistance. (Zulehner et al)

2.5.3 Quantum Dots

In order to produce silicon quantum dots, hydrogen silsesquioxane is thermally processed into nanocrystals with sizes ranging from a few nanometers to a few microns. These nanocrystals exhibit luminous qualities that depend on their size. Due to their low self-absorption, nanocrystals can be used in luminescent solar concentrators and quantum dot displays because they exhibit substantial Stokes shifts that convert photons in the ultra-violet range to photons in the visible or infrared, depending on the particle size. The non-toxic, metal-free characteristic of silicon makes it preferable to cadmium or indium for use in quantum dots. Hazardous substance sensing is another use for silicon quantum dots. By suppressing the photoluminescence in the presence of the dangerous material, the sensors take advantage of the luminous features of the quantum dots.

2.5.4 Human Nutrition

In studies showing that premenopausal women with higher dietary silicon intake have higher bone density and that silicon supplementation can increase bone volume and density in patients with osteoporosis, there is some evidence that silicon is important to human health for their nail, hair, bone, and skin tissues. One such study shows that premenopausal women with higher dietary silicon intake have higher bone density. Although silicon has been thought of as an essential element because it is necessary for the synthesis of elastin and collagen, the body's largest stores of which are found in the aorta, it is challenging to demonstrate this. This is because silicon is very common and, as a result, symptoms of a deficiency are difficult to reproduce.

2.6 OTHER SOURCES OF SILICA FOR PREPARATION OF SILICON VIA REDUCTION OF SILICA ROUTE

The existing industrial production process is costly and consumes a significant amount of energy. The fundamental manufacturing process involves heating high-quality quartz sand to temperatures between $1300^{O}C$ and $1600^{O}C$ and combining it with sodium carbonate (Begum et al., 2018). Therefore, there is a lot of research being done on how to make sodium silicate and precipitated silica from silica-rich industrial by-products. The recovery of silica from various ashes, including coal combustion ashes (Kaduku et al., 2015), biomass bottom ashes (Alam et al., 2019), rice husk ashes (Begum et al., 2018), pine cones and needles (Assefi et al., 2015), lemon grass ashes (Firdaus et al., 2016), sugarcane bagasse ashes (Channoy et al., 2018).

2.6.1 BIOMASS BOTTOM ASH

Bottom ash from the incineration of municipal solid waste is a silica-rich residue that, because to its high silica content and ease of accessibility, makes a useful starting point for the synthesis of sodium silicate. The total amount of bottom ash generated in the EU in 2014 was 18 million tonnes (Alam et al., 2017). Bottom ash is a difficult material to recycle because it is a complicated mixture of minerals that includes a range of impurities, including heavy metals (Alam et al., 2017). The ashes are being recycled in the form of loose aggregates, adsorbent ceramics (Bourtsalas et al., 2015), mixed cement (Li et al., 2012), and alkali activated materials, as mentioned by Luo (2017). (Silva et al., 2017). According to Alam (2018), silica recovery was done using bottom ash from municipal solid waste incineration. According to Liu et al. (2014), bottom ash may be used to extract silica by fusing it with $LiBO_2$ at 900 ºC. It is not well known how silica is extracted from rocks and how such changes in

mineral composition are related. Furthermore, silica dissolution from these cremation ashes at a low temperature would be preferable from an economic and environmental standpoint.

Figure 2.3 Biomass bottom-ash

2.6.2   WASTE GLASS CULLET

Waste glass cullet, which contains between 70 and 75 percent amorphous silica, has also been identified as a viable source of silicate, according to study done by Vinai (2019). Thermochemical or fusion techniques are used to produce low-cost, ecologically acceptable silicate solution from waste glass (Puertas, 2012). The process involves combining glass cullet and NaOH powders, and then heating the mixture to extremely high temperatures, such as 500°C, 650°C (Keawthun, 2014), and 700°C to 1300°C (Hu ,2015). The conversion of glass cullet to silica was high, but the resulting powder's solubility at ambient pressure was poor, necessitating warming at 175 °C for at least an hour and still not dissolving completely (Vinai & Soutsos, 2019).

Figure 2.4 Waste glass cullets

2.6.3   SAND

High purity silicon may be produced from natural resources such as sand (Ishmah et al., 2020). The solid-liquid extraction technique was employed in a 2020 study to create sodium silicate from beach sand. At 95°C, alkaline fusion of the beach sand precursors with NaOH produces Na_2SiO_3. The initial content examination in sand revealed that silica made up 69.87% of its composition, while other chemicals had lesser percentages, according to the research article (Ishmah et al., 2020). Sodium silicate, a precursor to the creation of silica, is often produced by melting quartz sand with sodium carbonate at 1300 °C, according to published research (Firdaus et al., 2016); (Chindaprasirt & Rattanasak, 2020); (Begum et al., 2018). The production process, however, is quite costly and uses a lot of energy.

Figure 2.5 Heap of sand

2.6.4   SUGARCANE BAGASSE

A high concentration of vital substances may be found in agricultural waste, such as sugarcane bagasse (Harish et al., 2015). When bagasse is burned, its silica-rich chemical makeup is disclosed by the ash that is produced (James & Pandian, 2017). Bagasse is the fibrous waste left over after the cane juice has been extracted from sugarcane. Bagasse ash offers an appealing substitute silica source for silica extraction due to its high silica concentration (Chindaprasirt, 2020). Alves (2017), Chindaprasirt (2020), Harish et al. (2015), and other research have suggested silica may be produced from sugarcane bagasse ash. Alkali extraction and acid precipitation are methods that use little energy and chemical input to produce sodium silicate and silica from bagasse ash.

Figure 2.6 Sugarcane bagasse
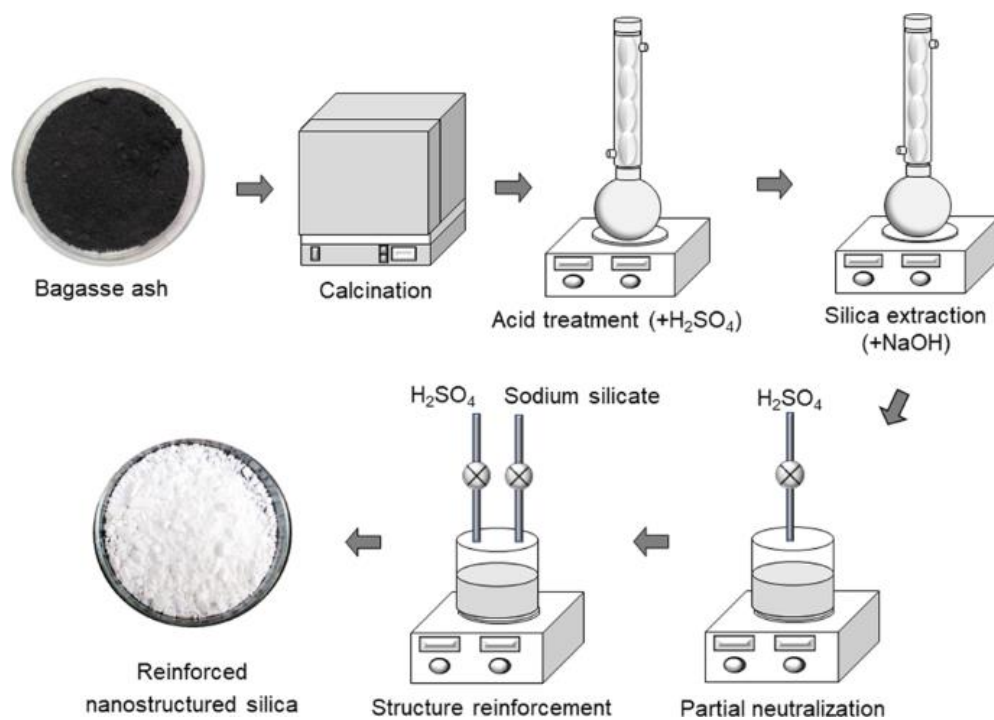
Figure 2.7 Process flow for the production of nano-silica particles from Rice husk ash via sodium silicate route

2.6.5   RICE HUSK ASH

Ash from rice husks, can be used to synthesize Silicon via the silica route. More than 90% of the silica in rice husk is active silica. Rice husk ash can include silica in the amorphous form, making it a potentially useful material for the production of silicon carbide, silicon nitride, and silica, according to a study by Niyomwas, S. (2017). Sodium hydroxide (NaOH) was utilized as an alkaline agent to extract silica since studies in the pilot plant study on synthesis of sodium silicate from rice husk ash (Begum et al., 2018) indicated that RHA is soluble in alkaline solution.

10% (by weight of all components) rice husk ash and 30% water were combined using the procedure in a clean stainless mixing vat. The mixture was heated at 1000 ºC for 10 minutes with 5% sodium hydroxide (NaOH) added. After then, the mixture was continually swirled while being diluted with 55% water. This phase involved letting the diluted solution sit at room temperature for a minimum of 24 hours without being disturbed. Decantation was used to remove the suspended solid from the dilute sodium silicate solution after it had set. It was heated to a point where the tiny suspended particles in the decant solution coagulated. After cooling the solution to room temperature, the coagulated mass became apparent. The coagulated substance was then separated by cloth filtration when enough time had passed. After evaporating the filtrate at a temperature of 1000 ºC, sodium silicate was produced.
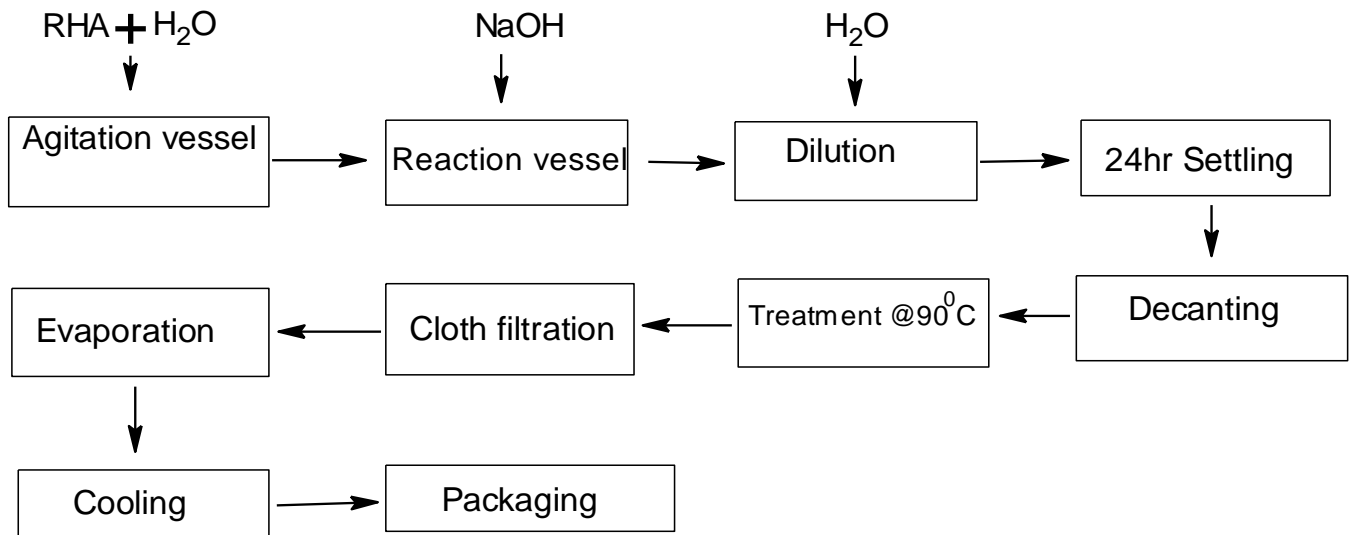
Figure 2.8 (a) rice husk (b) rice husk ash (c) un-sieved rice husk ash

2.6.6 LEMON GRASS

In a research carried out by Firdaus (2016), lemon grass biomass waste is a cheap raw material that can be utilized to manufacture natural silica, which can be used in the creation of silicon. It was discovered how to extract pure silica from lemon grass by first leaching it in hydrochloric acid (HCl),

then thermally combusting it at 600 °C. 98.58% was the reported silica yield figure, which is the highest yet (Firdaus et al., 2016).

 Figure 2.9 Lemon grass

2.6.7   COAL FLY ASH

It has been suggested that coal fly ash, an inorganic powder produced after the burning of coal, is a source of silica. Several studies have been conducted and reported on the beneficiation of coal fly ash, which includes lowering the risk of environmental contamination with heavy metals and also in applications for recovery of valuable components such as sodium silicate from fly ash were developed (Kaduku et al., 2015); (Miricioiu & Niculescu, 2020). According to Okoronkwo (2013), high silica concentration has also been found in coal fly ash made from various materials such rice husks, bagasse, and maize cobs. SiO_2 was recovered from coal fly ash and utilized as a starting material to synthesis sodium silicate, according to a study conducted in South Africa in 2015. (Wazamtu, et al.,2015). An enormous environmental issue arises from the disposal of the approximately 25 Mt of coal fly ash that is produced yearly in South Africa (Kaduku et al., 2015) hence use of coal fly ash as source of sodium silicate has a positive impact on the environmental disposal problem of coal fly ash.

Figure 2.10 Coal fly ash

2.7   CHARACTERIZATION METHODS FOR SILICON

2.7.1   TRANSMISSION ELECTRON MICROSCOPY (TEM)

The characterisation of nanocomposites has made extensive use of the transmission electron microscope, one of science's most potent tools (Kannan, 2018). It has the capacity to investigate the characteristics of these nanocomposites, such as grain size and shape, crystallinity, and chemical changes, at a resolution down to the nanoscale scale. Lattice flaws, atoms, and even their motions may be seen with the help of current TEM's superior design (Kohjiya et al., 2020). When a very thin sample is exposed to a high intensity electron beam, details such as the crystal structure and structural elements like dislocations and grain boundaries may be observed through the interactions between the electrons and the atoms. In order to assess the characteristics of quantum wells, wires, and dots, as well as their size, shape, and density, high resolution is used. Since electrons have a significantly shorter wavelength than light, their usage in TEM allows for pictures with an ideal resolution that is orders of magnitude higher than what can be achieved with a light microscope. TEM operates on the same fundamental principles as a light microscope (Kannan, 2018). The smallest features of interior structure, and sometimes even individual atoms, may therefore be shown by TEMs.
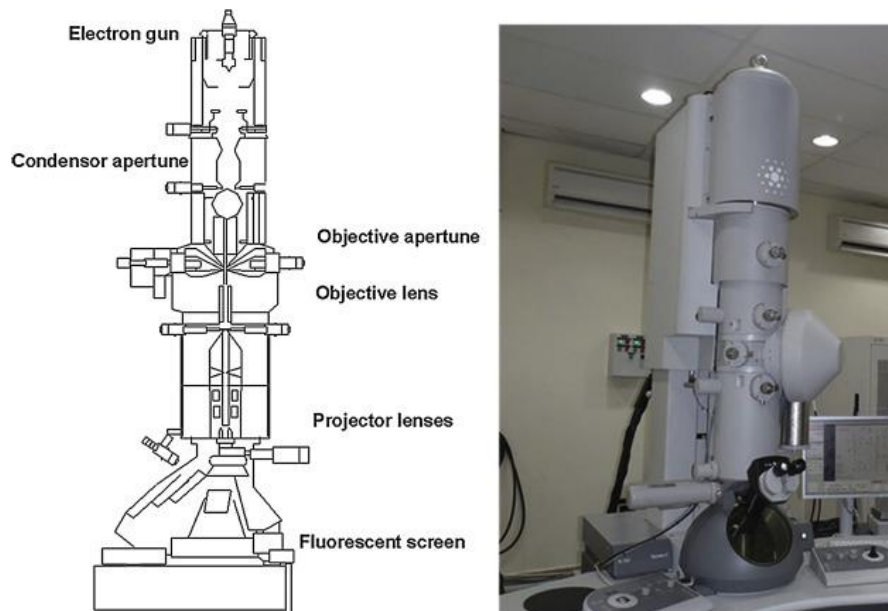
Figure 2.11 (a) Schematic representation of TEM (b) Representation of TEM instrumentation

2.7.2   SCANNING ELECTRON MICROSCOPY (SEM)

The electron column, the detecting system, and the viewing system are the three separate components that make up the SEM. The same scan generator concurrently controls two electron beams, one for the cathode ray tube screen and the other for the incoming electron beam. Through the use of enlarged, three-dimensional pictures of the surfaces of heterogeneous organic and inorganic materials, scanning electron microscopy may be used to characterize the exterior morphology of these materials on a

nanoscale (nm) to micrometer (m) scale. In the realm of material science, SEM is a potent instrument for analyzing and understanding the microstructures of materials (Scheu & Kaplan, 2012). The interaction of an incoming electron beam and the solid object is the foundation of the SEM theory. A wide range of emissions from the specimen can result from electron bombardment, including backscattered electrons, secondary electrons, Auger electrons, X-rays, visible photons, and more. In order to adjust the strength of the second electron beam, the incident beam is scanned line by line over the sample. The secondary electrons that come from this are then collected, identified, and amplified. Depending on the surface morphologies of the materials, a map of the brightness of secondary electron emission intensity from the scanned region of the sample will be displayed on the cathode ray tube screen (Akhtar, 2018). Using this method, it is possible to change the SEM image's magnification by only altering the size of the area that is being scanned on the sample surface. The diameter of the electron probe beam at the specimen surface has a significant impact on the spatial resolution of the SEM. Before it reaches the sample surface in a SEM system, the incident electron beam's diameter is demagnified using two or more electron lenses. The resolution of the SEM is also significantly influenced by the effective diameter of the electron source.
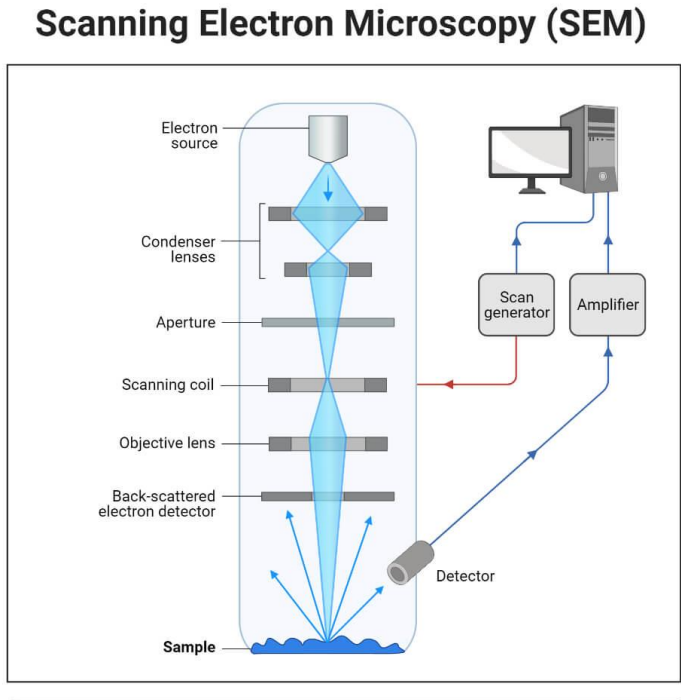
Figure 2.12 Schematic representation of SEM

2.7.3   FOURIER TRANSFORM INFRARED SPECTROSCOPY (FTIR)

Infrared radiation spectroscopy involves assembling absorption data and analyzing it in the form of a spectrum. Fourier Transform The technology of infrared spectroscopy (FTIR) is based on the vibrations of the atoms within a molecule. It is used to identify unidentified materials, assess the caliber or consistency of a sample, and calculate the proportions of the ingredients in a combination (Ganzoury et al., 2015). Infrared radiation flows through a material and is used to calculate the incoming radiation that is absorbed at a certain energy. The energy at which any peak in an absorption spectrum emerges relates to the frequency of a vibration of a sample molecule's component (Munajad et al., 2018). Additionally, chemical bonding will absorb different intensities and frequencies in various surroundings. It is possible to directly connect the incidences of infrared radiation absorption bands (also known as "peaks" or "signals") to the bonds present in the target chemical. Each interatomic link vibrates in a variety of stretching and bending movements, and individual bonds may absorb infrared light at more than one frequency. However, the weaker bending absorptions might be helpful in identifying comparable types of bonds from each other. Stretching absorptions often result in greater peaks than bending ones.
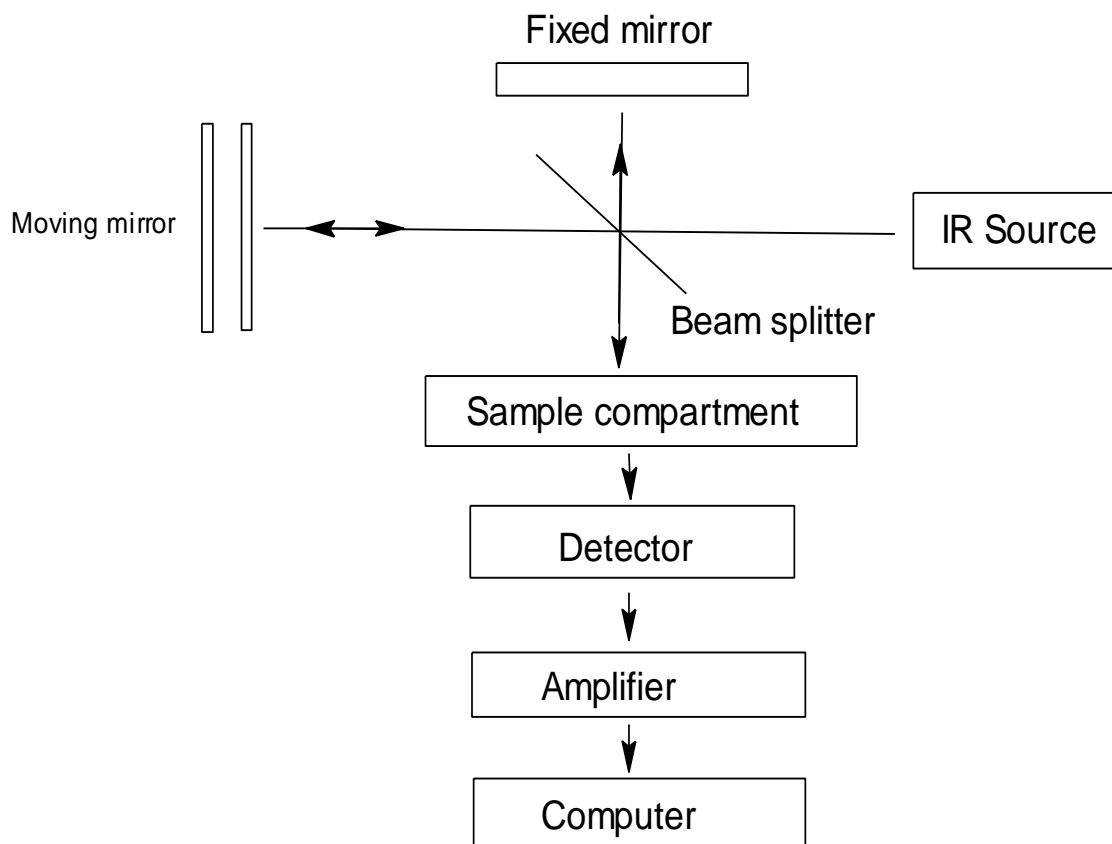
Figure 2.13 Schematic representation of working principle of the FT-IR

2.7.4   X-RAY POWDER DIFFRACTION (XRD)

The primary function of X-ray powder diffraction is to identify crystalline materials, and it can provide information about the size of unit cells (Dutrow & Clark, 2015). Constructive interference between monochromatic X-rays and a crystalline sample is the foundation of X-ray diffraction. A cathode ray tube produces the X-rays, which are then filtered to create monochromatic radiation, focused by collimation, and pointed towards the sample. When the circumstances are in accordance with Bragg's Law (n=2d sin), the interaction of the incident rays with the sample results in constructive interference and a diffracted beam. This rule connects the lattice spacing and diffraction angle of a crystalline sample to the wavelength of electromagnetic radiation (Bunaciu et al., 2015). Then, these diffracted X-rays are identified, examined, and tallied. Due to the powdered material's random orientation, all potential lattice diffraction directions should be obtained by scanning the sample over a range of 2 angles. Because each mineral has a specific set of d-spacings, converting the diffraction peaks to d-spacings enables mineral identification. Usually, this is accomplished by comparing the d-spacings with accepted reference patterns.
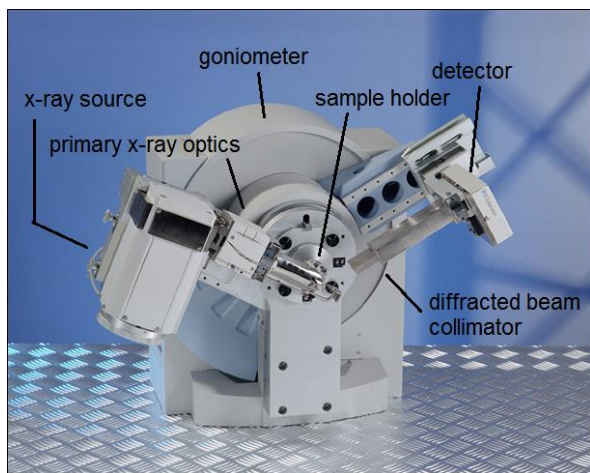
Figure 2.14 Diagram outlining XRD instrumentation

2.7.5   X-RAY FLUORESCENCE (XRF)

An analytical technique for both solid and/or liquid samples that is nondestructive, quick, and simultaneous with several elements is X-ray fluorescence (XRF) (Chen et al., 2018). One of the few atomic spectrometric techniques that can be used with field portable instrumentation is X-ray fluorescence, a method that has a long history of use in laboratories (Chen et al., 2018). Fluorescent x-rays are released from the sample as a result of a strong x-ray beam's irradiation. Either a wavelength- or energy-dispersive detector can pick up the x-rays that are being produced. The elements contained

in the sample are identified using either the energies or wavelengths of the produced x-rays, while the concentration of the elements is calculated by the intensity of the x-rays. The use of XRF technology has a number of benefits, including being one of the most straightforward, precise, and cost-effective analytical techniques for figuring out the chemical make-up of a variety of materials. It is trustworthy and non-destructive, requires little to no sample preparation, and works with solid, liquid, and powdered materials (Coccato et al., 2017)

Figure 2.15 Diagrammatic representation of XRF Instrumentation

CHAPTER 3: METHODOLOGY

3.1 INTRODUCTION

The major focus of this chapter is on the experimental techniques used to accomplish the research's objectives and aims. The steps are broken down into corn cob ash preparation, silica and silicon synthesis, sample methods and characterization techniques.

3.2 MATERIALS, REAGENTS AND EQUIPMENT USED

Table 3.1 Materials, Reagents and Apparatus

Reagents	Apparatus
❖ Sodium hydroxide ❖ Sulfuric acid ❖ Distilled water ❖ Corn cobs	❖ Muffle furnace ❖ Thermo Fischer Nicolet ᴛᴍIS5 FT-IR spectrophotometer ❖ pH meter ❖ Filter paper grade 4

The chemicals employed in this inquiry were analytical reagent grade, and all aqueous tests utilized distilled water and filter paper grade 4. To obtain corn cob ash, corn cobs were ashed in a laboratory muffle furnace. The sample's functional groups were identified using a Thermo Fischer Nicolet TMIS5 MIR FT-IR spectrophotometer, and drying was accomplished in an oven and a pH meter was used to assess the acidity or basicity of samples.

3.3 SAMPLING AND SAMPLE PREPARATION OF CORN COB ASH

The corn cobs used in this investigation was collected from a local farmer in Mazowe. Peeling off the corn kernels from the cobs and washing them with distilled water were done before they were dried in an oven overnight at 40°C. To achieve full burning, the dried corn cobs were broken into smaller pieces prior to any treatment. The dried corn cobs were burned in a laboratory biochar in open air. Ash content was measured for each heating temperature utilized in order to assess how temperature affected the amount of ash in corn cob. To homogenize the sample, the collected corn cob ash was first ground in a mortar and pestle and then filtered through a clear edge test sieve with a 250 μm aperture.

3.4 ACID LEACHING OF BURNT ASH AND EXTRACTION OF SILICA ASH

A 500 mL (1:5) w/v mixture of 1 M sulphuric acid solution (H_2SO_4) and 100 grams of weighed maize cob ash served as the starting point for the operation. The suspension was then refluxed and agitated for two hours at 70°C. Filter paper grade 4 was used to get the suspension, and 1500 mL of distilled water was used to wash the solid residue three times in order to thoroughly remove contaminants and metallic ions. The residue after washing was gathered and baked at 60°C. At 700°C, the dried corn cob ash was calcined till it became white. Alkaline treatment of corn cob ash has been shown to be a successful way for modifying the chemical and physical structure as well as for removing metal contaminants (Sahiron et al., 2017). The remaining maize ash was mixed in at a ratio of 1:5 w/v with a 3M sodium hydroxide solution. To create a sodium silicate solution, the mixture was aggressively agitated, boiled for two hours at 80°C, and the reaction duration was changed during the process. After that, a quantitative filter paper grade 4 was used to remove any remaining carbon from the solution. In order to create silica gel, the filtrate solution was gradually acidified by the addition of 1M H_2SO_4 while maintaining a pH range of 5.5 to 7.5. For the purpose of forming a gel-like material, the solution was aged for 24 hours. To create white silica powder particles, the gel was carefully cleaned with distilled water and dried.

```
┌─────────────────────────────────────┐
│        Peeling off corn kernels       │
└─────────────────────────────────────┘
                  │
                  ▼
┌─────────────────────────────────────┐
│      Drying in an oven at 40°C        │
└─────────────────────────────────────┘
                  │
                  ▼
┌─────────────────────────────────────┐
│    Devolatilization in muffle furnace │
└─────────────────────────────────────┘
                  │
                  ▼
┌─────────────────────────────────────┐
│ Grinding of corn cob ash using mortar and pestle │
└─────────────────────────────────────┘
                  │
                  ▼
┌─────────────────────────────────────┐
│               Sieving                 │
└─────────────────────────────────────┘
```
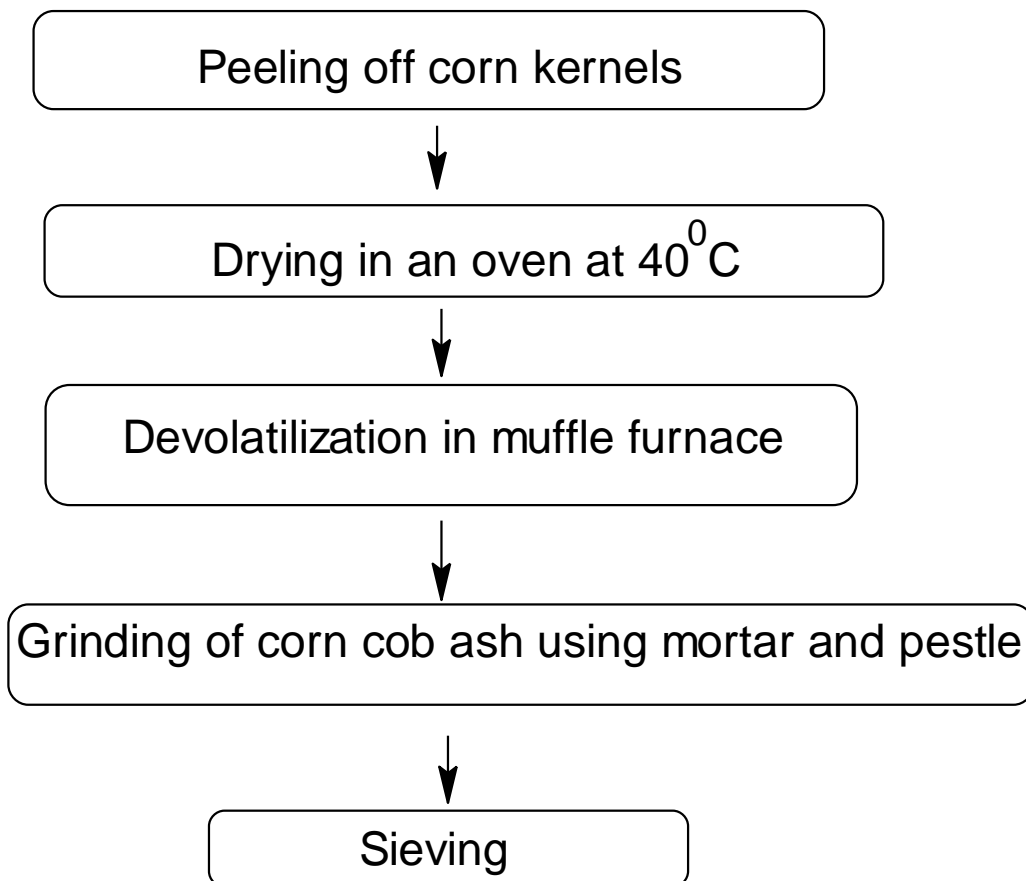
Figure 3.1 Steps taken in sample preparation of corn cob ashes

3.5 CHARACTERIZATION TECHNIQUES

3.5.1 ASH CONTENT DETERMINATION

Its mass was calculated by weighing an empty crucible and after being weighed, 50g of corn cob sample was added into crucible and the sample was ashed for three hours at various temperatures in a muffle furnace. Then, after cooling and being weighed once again with the ash within, the crucible was removed. A record was made of the ash's mass. The procedure was repeated in order to determine the ash concentration of corn cob ash produced from corn cob. Ash content was calculated according to the following equation;

$$\% \text{ Ash content} = \frac{\text{weight of corn cob ash}}{\text{weight of corn cob}} \times 100$$

3.5.2 MOISTURE ABSORPTION CAPACITY

Small container containing 3g of dried silica gel was placed in desiccator, which was then filled with 100 ml of water in a beaker to moisten the air. For five days, silica gel's weight change was monitored every day at the same time. To see the changes clearly, a graph showing the proportion of moisture absorbed over time in days was plotted. Moisture absorptive capacity was calculated using the equation below.

$$\text{Moisture Absorption Capacity} = \frac{\text{Increase in moist air absorbed}}{\text{weight of sample}} \times 100$$

3.5.3 BULK DENSITY

The silica gel's mass was calculated. By packing the silica powder particles into a column with a predetermined volume, volume was determined. For the purpose of determining corn cob ash, the process was repeated. The formulae below was used to calculate the bulk density;

$$\text{Bulk density} = \frac{\text{mass of sample}}{\text{volume of sample}}$$

3.5.4 INSTRUMENTAL METHOD

Figure 3.2 FT-IR instrumentation at the Bindura University chemistry lab

3.5.5 FOURIER TRANSFORM INFRARED SPECTROSCOPY ANALYSIS

The materials' functional group was identified using FTIR. On a molecular level, FTIR enables the identification of different types of linkages. To verify the identification of a pure substance or to find specific impurities, absorbed bands at a specified wavelength were utilized. The samples were pulverized into a fine powder and put onto an iD7-ATR-Diamond KBr for FTIR spectroscopy using a Nicolet Thermo Fisher, Germany FTIR to validate the structure of the silica gel. DTGS KBr detectors were used to create the spectra.

CHAPTER FOUR: RESULTS AND DISCUSSION

4.1 Introduction

This chapter chiefly focuses on the statistical, pictorial and graphical presentation and analysis of data and results obtained during the course of experimentation. The results to be presented were obtained from the synthesis, characterization of silica gel and silicon.

4.2 Pyrolysis and determination of ash content

Table 4.1 Ash content of corn cob

Temperature/^{o}C	700	800	900
Ash content/%	3.1	2.7	2.3

Table 0.2: Ash content of corn cob ash

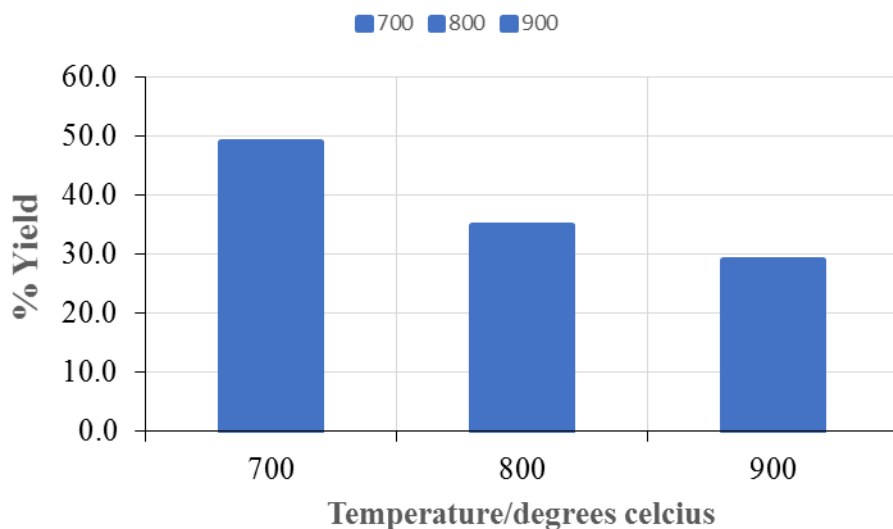| Temperature/^{o}C	700	800	900
Ash content/%	49	35	29

Figure 4.1 Outline of effects of temperature on ash content

To evaluate the influence of temperature on the ash and to determine the ash content, several temperatures were utilized. The measured ash was black at 600°C, indicating a substantial amount of unburned carbon. At temperatures of 700°C and 800°C, the color of the ash changed to grey and light

brown as shown in figure 4.1 above, indicating that there was less unburned carbon present. When corn cob ash is burned at high temperatures, the amount of carbon in the ash is considerably reduced. The mass of ash reduced as the temperature went from 600°C to 900°C, resulting in a decrease in ash content. Mass loss during ash ignition resulted in a significant decrease in the amount of ash produced. As can be seen in the graph above, corn cob ash had an ash content of 49%, 35%, 29%, and 700, 800, and 900 degrees Celsius, respectively. The ash concentration of pine ash decreased as temperature rose, but it was incredibly low at 800oC, which might be related to the high ignition temperature. At this high temperature, less carbon remains unburned, the weight of the ash entirely decreases, and the yield likewise decreased.

4.3 Determination of the time required to calcinate and its effects

Figure 4.2 Before calcination

Figure 4.3 Post calcination in muffle furnace at 600°C for 2 hours

Figure 4.4 Post calcination in muffle furnace at 900°C giving reddish-brown colour

Table 4.2 Calcination results showing varying calcination times in table below

Sample	1	2	3
Time taken to calcinate/hrs	2	3	4
Mass of ash before calcination/g	100	100	100
Mass of ash post calcination/g	52,418	45,243	34,821
Percentage yield of ash/%	52,4	45,2	35,0

The calcination temperature was adjusted to 700°C to produce the most ash. In order to stop impure silica from developing, calcination was used to remove unburned carbon and organic waste from the ash. The ash's color shifted from black to grey and then from grey to red-brown, indicating that there was much less unburned carbon present. Different calcination times ranging from 4 to 2 hours were used to test how time affected the process. The mass of ash recovered at 3 hours was greater than the mass of ash collected after 4 hours. The ash production dropped to 29% after 4 hours of calcination. This indicates that as the calcination period lengthens, the mass of ash decreases.

4.4   Alkaline extraction and Acid Precipitation
Table 0.1: Results of alkaline extraction and acid precipitation

Sample	1	2	3
Volume of NaOH used/cm^3	500	500	500
Volume of NaOH used/cm^3	642	510	294
Volume of NaOH used/cm^3	592	575	361
pH	7,92	7,36	8,17

Figure 4.5 Gelation process

4.5 Effect of pH, aging time and silica gel yield

Table 0.2: Results of effect of pH, aging time and yield

Sample	1	2	3
pH	7,92	7,36	8,17
Aging time /hours	24	48	72
Mass of silica gel obtained/g	2,94	6,15	7,86

According to the table, silica gel output fell at pH 7.92 and increased at pH 8.17. The formation of silica gel decreased when the pH approached 8,17. According to Wilhelm and Kind (2015), the reaction progresses quickly at high pH levels, rapidly depleting the reaction in solution. Time-delayed gelation

unstable sols can develop at pH values of 8 to 10 and 2 to 5, while pH levels of 5 to 8 cause silica to gel most quickly. The table demonstrates how the amount of time the gel is aged has an impact on its yield of silica gel, with the yield rising as the aging time does. The gel complex then continues to change as the gelation process progresses, increasing the gel strength gradually. As the system gets closer to equilibrium, syneresis takes place when the gel contracts and expels the liquid it is holding. Most of the time, syneresis is caused by the condensation of two silanol groups during the gelation process, which results in the formation of new bonds, specifically siloxane linkages (–Si–OH). Gel shrinkage happens because, as Wilhelm & Kind (2015) pointed out, the siloxane bond that was produced requires less space than the two distinct silanol groups from which it was derived.

Figure 4.6 Silica gel samples post drying

4.6 Moisture Absorption Capacity
Table 0.3: Moisture absorption of sample 1

Day	Initial	1	2	3	4	5
Moisture gained/gday^{-1}	0,00	0,43	0,36	0,33	0,29	0,24
% moisture gained	0,00	9,20	17,40	26,10	33,20	36,70

Table 0.4: Moisture absorption of sample 2

Day	Initial	1	2	3	4	5
Moisture gained/gday^{-1}	0,00	0,44	0,42	0,38	0,36	0,28
% moisture gained	0,00	9,50	19,70	28,20	35,90	39,20

Table 0.5: Moisture absorption of sample 3

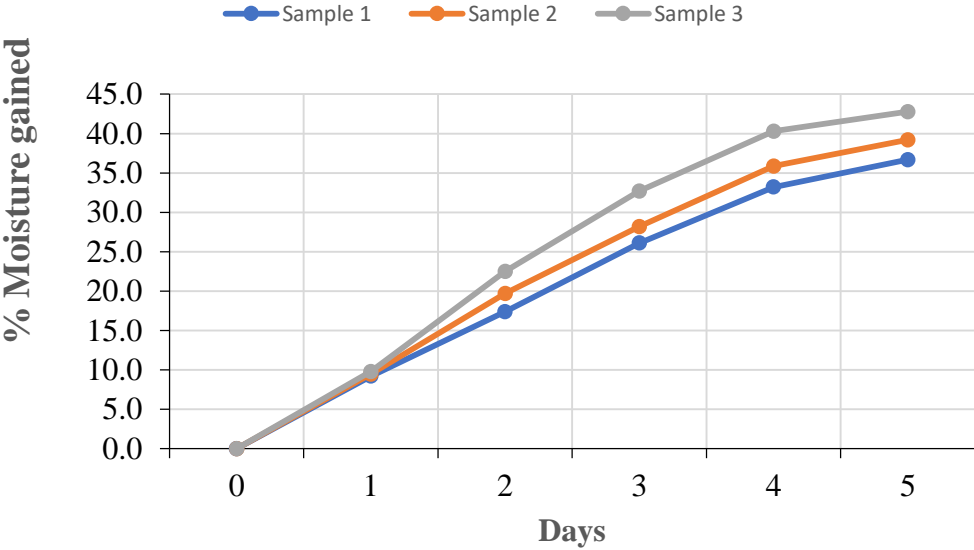| Day	Initial	1	2	3	4	5
Moisture gained/gday^{-1}	0,00	0,45	0,41	0,38	0,35	0,27
% moisture gained	0,00	9,80	22,50	32,70	40,30	42,80

Figure 4.7 Graph of moisture absorption

The above chart illustrates the amount of moisture absorbed overall has increased for samples 1, 2, and 3. Sample 3 has the largest absorption capacity, while Sample 1 has the lowest. The rate of moisture absorption steadily reduces with time, in accordance with the kinetics of water vapour adsorption, after initially being high. For gels that have been aged for extended periods of time, a decrease in surface area is assumed to be responsible for the decline in adsorption ability. The ability of a desiccant to absorb moisture is a crucial feature. Choiril (2019) claims that the gel's huge surface area is what gives

it its great adsorption capacity. Because silica gel has a large specific surface area, it can quickly absorb water, which makes it a superior drying agent. The outcomes demonstrate that the preparation method was effective in creating silica particles with a high specific surface area and enhanced moisture absorption capability.

4.7 Determination of bulk density

Table 0.6: Bulky density of corn cob ash

Mass of ash/g	5,80
Volume of ash/ cm^{-3}	9,90
Bulk density g/cm^{-3}	0,5858
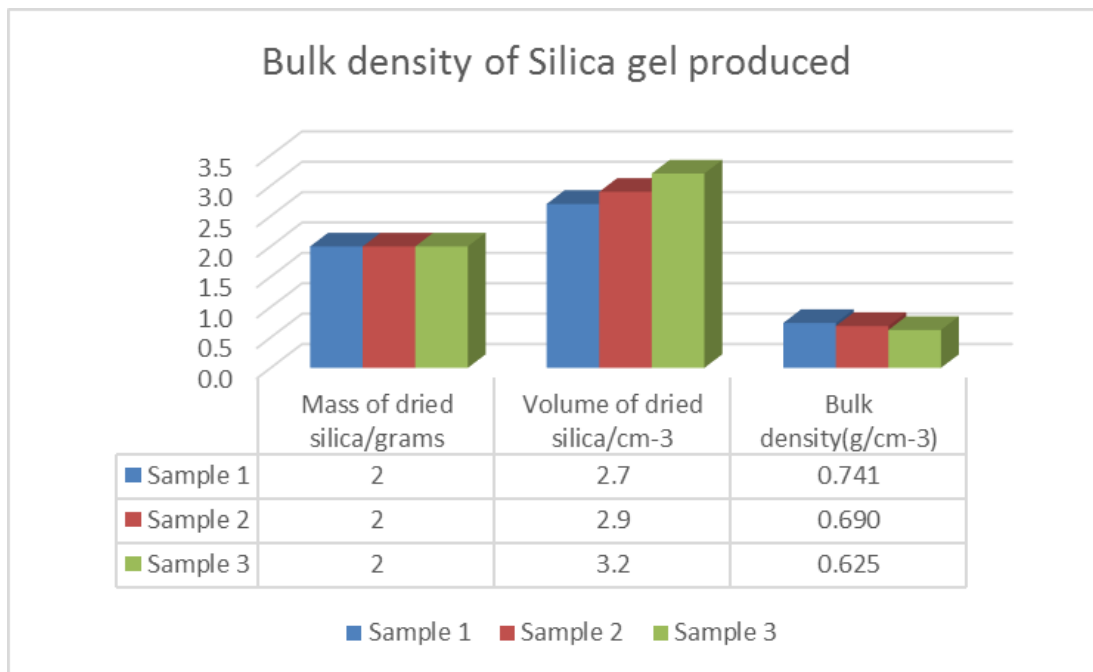
Figure 4.8 Bulk density graph

The results for the bulk densities of the silica gel and corn cob ash samples are shown above, respectively. For maize cob ash, the bulk density was 0.5858 g cm^3. Bulky densities for the three silica samples were 0.741, 0.690, and 0.625 gcm^{-3}, respectively. Bulky density is defined as solid particle weight per unit solid particle volume. Pore space within the sample diminishes as bulky density rises.

The sample's particles are more likely to be free the lower the bulky density, and more likely to be compressed the higher the bulky density.

4.8 Reduction of silica gel and silicon yield

Table 0.7: Results for reduction of silica gel and silicon yield

Sample	1	2	3
Ratio of SiO_2:Mg (w/w)	1,5	3,2	3,2
Mass of silica used (grams)	10	10	10
Mass of silicon produced	17	19	15

The high amount of silicon that was formed by the silica and Magnesium's 1:5 dissolution ratio may have been caused by the sample's high water content and poor viscosity. The samples 2 and 3 produced identical amounts of silicon, according to the dissolution ratio of 3:2 (w/w) for silica to hydroxide. Since there was less water in both samples than in sample 1, the sodium silicate was more viscous in both. Because silica enhances the viscosity of the sodium silicate solution, using a 3:2 ratio for silica to hydroxide is more effective than using a 1:5.

4.9 Percentage yield of silica gel and silicon

Table 0.8: Results for yield of silica gel and silicon

Sample	1	2	3
Silica gel/g	20	20	20
Silicon/g	13	17	16

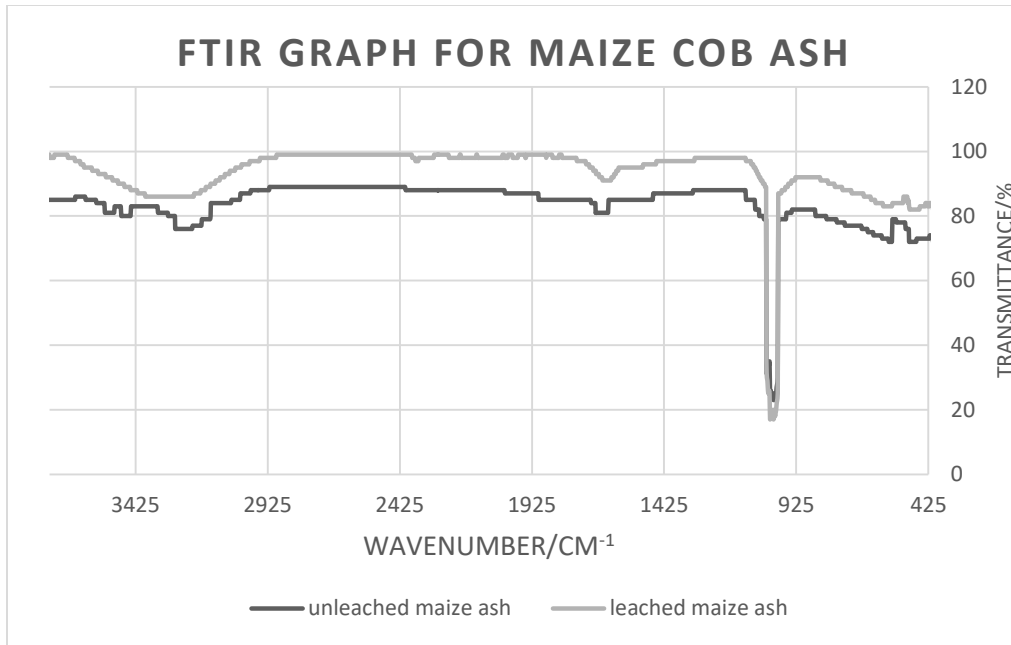## 4.10 Spectra of silica gel and silicon

Figure 4.9 FTIR Spectra for leached and un-leached corn cob ash

The sample of un-leached maize cob ash's FTIR spectrum is displayed in Fig. 4.6 in the range of 4100-300cm-1. Peak is visible in the spectra at 972 cm-1. Si-O bending from Si-O-Si bending is attributed to the peak at 413. Si-O-asymmetric Si's vibrations are attributed to the absorption peak at 972 cm-1. Un-leached ash displayed a strong band wavenumber of roughly 1000cm-1, indicating the presence of silica.
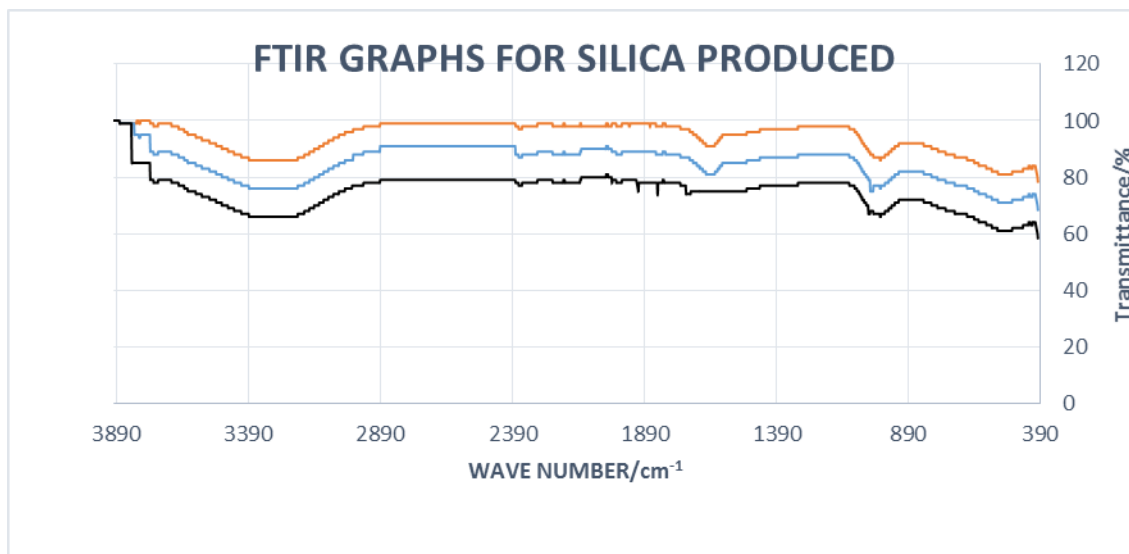

Figure 4.10 FTIR Spectra for silica samples produced from different parameters

Sample 1 represented by black line ----

Sample 2 represented by blue line ----

Sample 3 represented by red line ----

Figure 4.7 shows the FTIR analysis results of silica gel samples. The spectrum indicate that all the three samples have peaks at around 1000 cm^{-1} which confirms the presence of silica. The spectrum of sample 1,2 and 3 did not show any peaks around 3000 cm^{-1} which means no water is absorbed. These Si-O-Si absorption bands are typical of silica gels and have also been observed by various researchers. In sample 3 a peak that was absorbed at around 3390 cm^{-1} that some water molecules (OH) was trapped inside the silica matrix. However, for sample 3 a peak that was detected peak at about 1388 cm^{-1} may be associated with C=C aromatic indicating presence of carbon which may be due to carbon residue in the sample (Bunaciu et al., 2015). The peak detected at about 2980 cm^{-1} in sample 2 was associated with C-H indicating the presence of carbon residues in the sample produced. As indicated by the FTIR analysis results sample 1 and 2 was pure indicating it had insignificant amounts of carbon.
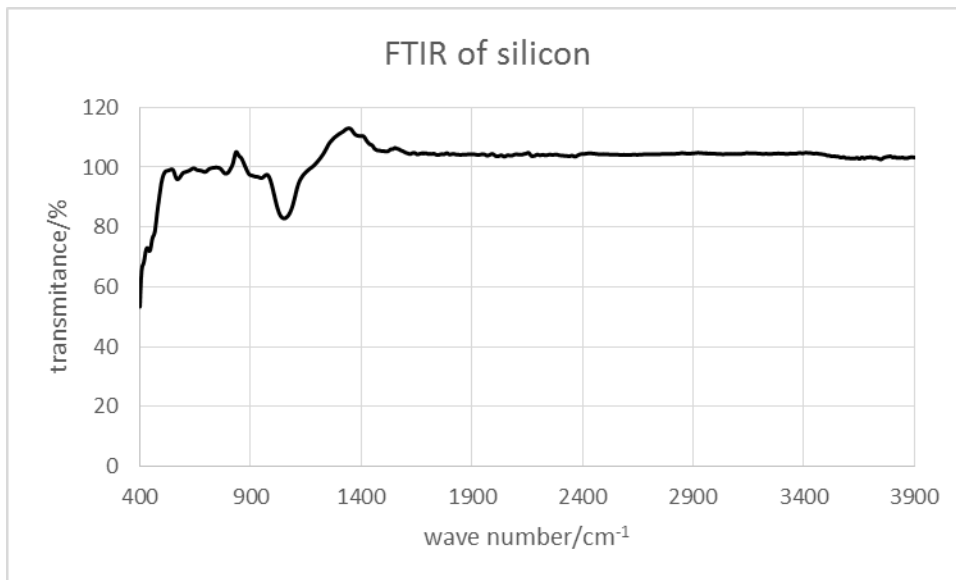

Figure 4.11 FTIR Spectra for Silicon produced

CHAPTER 5: CONCLUSION AND RECOMMENDATIONS

5.1 Recommendations

In the course of the acid leaching procedure, in order to determine how changing reaction circumstances impacts the chemical makeup of the ash, the researcher advises using a wider range of sulphuric acid concentrations. Additionally, the researcher advises employing tools to compare the chemical composition of ash before and after the leaching procedure. It is necessary to use TEM, SEM, and XRD to analyze the silica gel produced during the synthesis of silicon in order to determine the chemical content and morphology of the silica particles created. An elemental analyzer should be taken into consideration for the assessment of carbon residues present in silica gel prior to the reduction process for silicon production. In order to increase the effectiveness of raw materials other than corn cob ashes, the student advises that a pilot study of this research be carried out.

5.2 Conclusion

The findings of this study show that the methods created for producing silicon from corn cob ash were a beneficial and effective way to produce silica gel and silicon. Since Si-O-Si was present in every silica gel sample, it was clear that the material had been expertly manufactured from corn cob ash. Since the silica particles formed by acid leaching were completely white, it turned out to be a superb approach for removing the majority of the metallic contaminants. Silica that had been extracted using an alkaline technique and then reduced with a metal was used to make silicon. It was found that the method for silica extraction from corn cob ash was quick and easy. This study discovered that by separating silica from corn cob ash, it is possible to produce silicon, a valuable product with a wide range of applications, while simultaneously reducing the environmental impact of ash and maize cob disposal difficulties.

References

Ajayi B.A., Owoeye S.S. (2015). Extraction of Soluble Sodium Silicate using Corn Cob Ash as a Silica Source. *American Journal of Engineering Research (AJER). 54-56*

F. Latif, B.I. Rajoka (2014), Production of ethanol and xylitol from corn cobs by yeast. *Bio- resource Technology,* 77, 57-63.

Schollbach E., & Brouwers, F (2019). *Extraction of Silica from Burnt Paddy Husk. June*, 5–10.

G. Garrote, H. Dominguez, and J.C. Parajo, Hydrothermal processing of lignocellulosic materials. *Holz als Roh- und Werkstoff*, 57, 191-202.

W.J. Byung, C.H. Kim, G.H. Tae, and J.B. Park, Characteristics of cement mortar with nano-Silica particles, *Const. Build.Mater.,* 21, 2017, 1351-1355.

S.R. Kamath, and A. Proctor (2018), Silica gel from rice husk ash: preparation and characterization, *Cereal Chemistry,* 75, 484-487.

K. Mohanraj, S. Kannan, S. Barathan, and G. Sivakumar, Preparation and characterization of nano-Silica from corn cob ash by precipitation method. Optoelectronics and Advanced Materials- Rapid Communication*,* 6(3-4), 2012, 394-397.

Prasad, R., & Pandey, M. (2012). Rice husk ash as a renewable source for the production of value added silica gel and its application: An overview. In *Bulletin of Chemical Reaction Engineering and Catalysis* (Vol. 7, Issue 1). https://doi.org/10.9767/bcrec.7.1.1216.1-25

Wang, D., Zhang, J., Yang, Q., Li, N., & Sumathy, K. (2014). Study of adsorption characteristics in silica gel-water adsorption refrigeration. *Applied Energy*, *113*. https://doi.org/10.1016/j.apenergy.2013.08.011

Handayani L, S Aprilia, Abdullah, C Rahmawati, A M Mustafa Al Bakri, I H Aziz, E. A. A. (2021). Synthesis of Sodium Silicate from Rice Husk Ash as an Activator to Produce Epoxy-Geopolymer Cement Synthesis of Sodium Silicate from Rice Husk Ash as an Activator to Produce Epoxy-Geopolymer Cement. *Journal of Physics:Conference Series*. https://doi.org/10.1088/1742-6596/1845/1/012072

Kaduku, T., Daramola, M. O., Obazu, F. O., & Iyuke, S. E. (2015). Synthesis of sodium silicate from South African coal fly ash and its use as an extender in oil well cement applications. In *Journal of the Southern African Institute of Mining and Metallurgy* (Vol. 115, Issue 12, pp. 1175–1182). https://doi.org/10.17159/2411-9717/2015/v115n12a5

Liu, Y. M., Yuan, Z. X., Wen, X., & Du, C. X. (2021). Evaluation on performance of solar adsorption cooling of silica gel and SAPO-34 zeolite. *Applied Thermal Engineering*, *182*. https://doi.org/10.1016/j.applthermaleng.2020.116019

Megawati, Fardhyanti, D. S., Artanti Putri, R. D., Fianti, O., Simalango, A. F., & Akhir, A. E. (2018). Synthesis of Silica Powder from Sugar Cane Bagasse Ash and Its Application as Adsorbent in Adsorptive-distillation of Ethanol-water Solution. *MATEC Web of Conferences*, *237*, 1–6.https://doi.org/10.1051/matecconf/201823702002

Ma, H., Zhu, H., Yi, C., Fan, J., Chen, H., Xu, X., & Wang, T. (2019). Preparation and reaction mechanism characterization of alkali-activated coal gangue-slag materials. *Materials*, *12*(14), 16. https://doi.org/10.3390/ma12142250

Martinez-Hernandez, E., Amezcua-Allieri, M. A., Sadhukhan, J., & Anell, J. A. (2018). Sugarcane Bagasse Valorization Strategies for Bioethanol and Energy Production. In *Sugarcane - Technology and Research*. https://doi.org/10.5772/intechopen.72237

Mupa, M., Hungwe, C. B., Witzleben, S., Mahamadi, C., & Muchanyereyi, N. (2015). Extraction of silica gel from Sorghum bicolour (L.) moench bagasse ash. *African Journal of Pure and Applied Chemistry*, *9*(2), 12–17. https://doi.org/10.5897/ajpac2015.0603

Nandiyanto A B D, T Rahman , M A Fadhlulloh , A G Abdullah, I. H., & Mulyanti, and B. (2021). Synthesis of silica particles from rice straw waste using a simple extraction method Discover the world ' s research Synthesis of silica particles from rice straw stra w waste

using a simple extraction method The Potential Anticancer Activity of 5-Fluorou. *IOP Conference Series: Materials Science and Engineering PAPER*, 128. https://doi.org/10.1088/1757-899X/128/1/012040

R. Novotny, A. Hoff, and J. Schuertz (2021). Process for hydrothermal production of sodium silicate solutions, United States Patent, 5,000, 933.

N. Thuadaij, and A. Nuntiya (2018). Synthesis and characterization of nanosilica from rice husk ash prepared by precipitation method. Chiang Mai, J. Sci, 35, 206.

Sultana, M. S., Rahman, M. A., Zaman, M. N., & Ahmed, A. N. (2015). Influence of Calcination on Different Properties of Sugarcane Bagasse and Waste Ash. *JOURNAL OF SCIENTIFIC RESEARCH*, *7*(3), 151–157.

Adebisi, J. A., Agunsoye, J. O., Bello, S. A., Haris, M., Ramakokovhu, M. M., Daramola, M. O., & Hassan, S. B. (2016). *Extraction of Silica from Cassava Periderm using Modified Sol-Gel Method*. 57–65.

Chindaprasirt, P., & Rattanasak, U. (2020). Eco-production of silica from sugarcane bagasse ash for use as a photochromic pigment filler. *Scientific Reports*, *10*(1), 1–8. https://doi.org/10.1038/s41598-020-66885-y

Wilhelm, S., & Kind, M. (2015). *Influence of pH , Temperature and Sample Size on Natural and Enforced Syneresis of Precipitated Silica*. *November*, 2504–2521. https://doi.org/10.3390/polym7121528

Wazamtu, I., Sani, N. A., & Abdulsalam, A. K. (2013). Extraction and Quantification of Silicon From Silica Sand Obtained From Zauma River, Zamfara State, Nigeria. *European Scientific Journal*, *9*(15), 160–168.

Apelian, D. (2019). *"Aluminum Cast Alloys: Enabling Tools for Improved Performance"* . Wheeling, Illinois: North American Die Casting Association

Eranna, Golla (2014). *Crystal Growth and Evaluation of Silicon for VLSI and ULSI*. CRC Press. p. 7. ISBN 978-1-4822-3281-3

Kamal, Kamal Y. (2022). "The Silicon Age: Trends in Semiconductor Devices Industry". *Journal of Engineering Science and Technology Review*. **15** (1): 110–115.

Dekker, R; Usechak, N; Först, M; Driessen, A (2018). "Ultrafast nonlinear all-optical processes in silicon-on-insulator waveguides". *Journal of Physics D*. **40** (14): R249–R271

"CDC – NIOSH Pocket Guide to Chemical Hazards – Silicon". www.cdc.gov.

Science Lab.com. "Material Safety Data Sheet: Silicon MSDS". *sciencelab.com*